Ultra-light dark matter in ultra-faint dwarf galaxies

Erminia Calabrese[1,2]★ and David N. Spergel[1]

[1]*Department of Astrophysical Sciences, Peyton Hall, Princeton University, 4 Ivy Lane, Princeton, NJ 08544, USA*
[2]*Sub-department of Astrophysics, University of Oxford, Denys Wilkinson Building, Oxford OX1 3RH, UK*

ABSTRACT

Cold Dark Matter (CDM) models struggle to match the observations at galactic scales. The tension can be reduced either by dramatic baryonic feedback effects or by modifying the particle physics of CDM. Here, we consider an ultra-light scalar field DM particle manifesting a wave nature below a DM particle mass-dependent Jeans scale. For DM mass $m \sim 10^{-22}$ eV, this scenario delays galaxy formation and avoids cusps in the centre of the dark matter haloes. We use new measurements of half-light mass in ultra-faint dwarf galaxies Draco II and Triangulum II to estimate the mass of the DM particle in this model. We find that if the stellar populations are within the core of the density profile then the data are in agreement with a Wave Dark Matter model having a DM particle with $m \sim 3.7$–5.6×10^{-22} eV. The presence of this extremely light particle will contribute to the formation of a central solitonic core replacing the cusp of a Navarro–Frenk–White profile and bringing predictions closer to observations of cored central density in dwarf galaxies.

Key words: galaxies: dwarf – galaxies: haloes – cosmology: theory – dark matter.

1 INTRODUCTION

The Λ cold dark matter (ΛCDM) model emerged in the last two decades as the simplest model that consistently accounts for most astrophysical and cosmological observations (Spergel et al. 2003; Planck Collaboration XIII 2015). In this scenario, most of the matter content of the Universe is in the form of a non-interacting and non-relativistic matter component, Cold Dark Matter (CDM), and at present its nature is unknown.

CDM models successfully reproduce the evolution of a smooth early Universe into the cosmic structures observed today on a wide range of redshifts and scales. However, the agreement between models and observations degrades rapidly when zooming into the innermost galactic regions.

In the standard model of galaxy formation, galaxies are seeded by dark matter haloes (White & Rees 1978; Blumenthal et al. 1984; White & Frenk 1991), whose structure is a very powerful probe to distinguish between different theoretical models. DM haloes have been extensively studied with *N*-body simulations (see e.g. Kuhlen, Vogelsberger & Angulo 2012 for a review) and the similarities between different CDM-only simulated haloes have justified the definition of a universal dark matter halo profile, the Navarro–Frenk–White (hereafter NFW, Navarro, Frenk & White 1996) profile. However, improved resolution in *N*-body simulations has revealed that at small scales the CDM paradigm presents three major problems (see Weinberg et al. 2013 and references therein): (i) the

cusp-core problem – NFW density profiles arising from CDM-only simulations predict a steeper density (cusp) towards the centre of the DM halo compared to disc and dwarf spheroidal galaxies observations of a flatter central density (core); (ii) the missing satellites problem – CDM models predict more-than-observed Milky Way satellite galaxies living in DM sub-haloes; (iii) the too-big-too-fail problem – CDM models predict more-than-observed massive DM sub-haloes.

These problems can be solved at the theory level with two possible approaches: including baryonic feedback or other astrophysical effects into the simulations (see e.g. Governato et al. 2012; Di Cintio et al. 2014; Pontzen & Governato 2014; Oñorbe et al. 2015; Papastergis & Shankar 2015; Pawlowski et al. 2015, for recent discussions), or modifying the CDM component.

Here, we take the latter approach and consider a modification of the particle physics of DM, allowing for the presence of a light bosonic, axion-like, dark matter particle. If the DM particle is ultra-light, with mass $\sim 10^{-22}$ eV, than its wave nature can manifest on astrophysical scales and bring theoretical predictions closer to the observations (Goodman 2000; Hu, Barkana & Gruzinov 2000; Marsh & Silk 2014; Schive, Chiueh & Broadhurst 2014a; Schive et al. 2014b).

Ultra-light axion-like particles are one of the most compelling candidates for CDM and have been explored with different observables covering many cosmic epochs [from cosmic microwave background (CMB) data (Hlozek et al. 2015), Lyman α systems (Amendola & Barbieri 2006), reionization history (Bozek et al. 2015; Sarkar et al. 2016; Schive et al. 2016), and galaxy formation and dwarf galaxy dynamics (Lora & Magaña 2014; Schive et al.

2014a; Lora 2015; Marsh & Pop 2015)]. Axions will behave like matter in the present Universe as long as their mass is $>10^{-33}$ eV and consistency with the CMB demands that the dominant DM component has $m > 10^{-24}$ eV (Hlozek et al. 2015). On the other end, axions can feasibly be distinguished from CDM as long as $m < 10^{-18}$ eV (Marsh 2015b); heavier axions are allowed as DM, but are indistinguishable from CDM in their effects on structure formation. Collecting all cosmological and astrophysical information, we then currently know that $10^{-24} < m < 10^{-18}$ eV. See Marsh (2015a) for a comprehensive review.

To add to these DM mass constraints here, we consider two recently discovered ultra-faint dwarf galaxies in the Milky Way, Draco II, and Triangulum II (Laevens et al. 2015a,b). Both objects seem to be very peculiar. The analysis of Martin et al. (2016a) classifies Draco II as the smallest dwarf galaxy ever confirmed. Triangulum II is bigger than Draco II but fainter. Its nature is still controversial (see discussion in Kirby et al. 2015 and Martin et al. 2016b) but preliminary data reductions suggest it is likely to be a dwarf galaxy. In particular, it seems to be the dwarf with the largest mass-to-light ratio and so the most DM-dominated object ever observed. These two galaxies will complement existing constraints on DM.

The paper is organized as follows. We describe the Wave Dark Matter model in Section 2 and the data in Section 3. In Section 4, we estimate the DM particle mass and compare the predictions with a ΛCDM NFW model. We discuss our results and conclude in Section 5.

2 WAVE DARK MATTER HALOES

An alternative to CDM that has recently gained much attention is the Bose–Einstein condensate scalar field dark matter model (see e.g. Turner 1983; Ji & Sin 1994; Lee & Koh 1996; Guzmán, Matos & Villegas 1999; Goodman 2000; Matos, Guzmán & Ureña-López 2000; Böhmer & Harko 2007; Sikivie & Yang 2009; Woo & Chiueh 2009; Lundgren et al. 2010; Chavanis 2011, 2012; Chavanis & Delfini 2011; Harko 2011a,b; Harko & Madarassy 2012; Harko & Mocanu 2012; Lora et al. 2012; Magaña & Matos 2012; Harko 2014; Li, Rindler-Daller & Shapiro 2014; Lora & Magaña 2014; Suárez, Robles & Matos 2014; Davidson 2015; Guth, Hertzberg & Prescod-Weinstein 2015; Guzmán & Lora-Clavijo 2015; Harko & Lobo 2015; Harko et al. 2015; Lora 2015; Marsh & Pop 2015 and references therein), also known as Fuzzy Dark Matter (Hu et al. 2000) or Wave Dark Matter (Schive et al. 2014a). In this scenario, DM is made of extremely light bosons, such as axion-like particles, non-thermally generated and described by a scalar field ψ. If the field's bosons are ultra-light, with a mass $\sim 10^{-22}$ eV, quantum pressure from the bosons occupying the same ground state counters gravity and in the early Universe they condensate in a single coherent macroscopic wave (a self-gravitating Bose–Einstein condensate). The field is minimally coupled to gravity and interacts only gravitationally with the baryonic matter. In the Newtonian approximation and in the case of negligible self-interaction between bosons (as in the case presented in Hu et al. 2000 and Schive et al. 2014a that we will follow here), the scalar field is then well described by the coupled Schrödinger and Poisson equations (see e.g. Widrow & Kaiser 1993) and DM haloes are the ground-state solution – the gravitational configuration in equilibrium – of the system.

A very interesting feature of this model is an effective Jeans scale depending on the DM particle mass below which the uncertainty principle counters gravity. Galactic haloes form by the usual gravitational instability but with perturbations suppressed below a scale that is set by the particle mass. As a result, interestingly for galaxy formation, for $m \sim 10^{-22}$ eV flat (cored) density profiles are produced within $\sim 0.1 - 1.0$ kpc, galaxy formation is delayed and the halo mass function shows suppression of haloes smaller than $\sim 10^{10}$ M$_\odot$, helping with both the cusp-core and missing satellites problems (Goodman 2000; Hu et al. 2000; Marsh & Silk 2014; Schive et al. 2014a, 2016).

In this work, we consider the Wave Dark Matter model, ψDM, presented in Schive et al. (2014a,b). Schive et al. (2014a) performed the first high-resolution cosmological simulations for Wave Dark Matter and showed that the central density profiles of all collapsed objects are well described by the stable soliton solution of the Schrödinger–Poisson equation. A gravitationally self-bound soliton core is found in every halo superposed on an NFW profile. The NFW behaviour is recovered at larger radii and the ψDM cosmology is indistinguishable from CDM on large scales.

Fitting cosmological simulations, Schive et al. (2014a) shows that the density profile of the innermost central region at redshift 0 is well approximated by

$$\rho_s(r) = \frac{1.9(10m_{22})^{-2}r_c^{-4}}{[1 + 9.1 \times 10^{-2}(r/r_c)^2]^8} 10^9 \text{ M}_\odot \text{ kpc}^{-3}, \quad (1)$$

where $m_{22} \equiv m/10^{-22}$ eV is the DM particle mass and r_c is the core radius of the halo. The soliton extends up to $\sim 3r_c$ (Schive et al. 2014a,b).

From the density profile, we can estimate the enclosed mass at a given radius r:[1]

$$M(<r) = \int_0^r 4\pi\rho_s(r')r'^2 dr'. \quad (2)$$

$M_c \equiv M(<r_c)$ gives the central core mass and the total soliton mass will be $\sim 4M_c$.

Schive et al. (2014b) also derive an analytical dependence between the core mass or radius and the total mass of the halo, M_h, hosting the galaxy. At the present time these relations are:

$$M_c \sim \frac{1}{4} M_h^{1/3} \left(4.4 \times 10^7 m_{22}^{-3/2} \right)^{2/3}, \quad (3)$$

$$r_c \sim 1.6 m_{22}^{-1} \left(\frac{M_h}{10^9 \text{ M}_\odot} \right)^{-1/3} \text{ kpc}, \quad (4)$$

so that, for a given m_{22}, the largest cores are embedded on the smallest haloes.

For our purposes, the soliton is the only component of the density profile that compares to the data. We assume that the stellar populations are within the core and we do not need any extrapolation to NFW at larger scales.[2]

3 ULTRA-FAINT DWARF GALAXIES

Dwarf galaxies are believed to be the most common type of galaxies in the Universe. In a hierarchical formation scenario, these objects are the building blocks of more massive galaxies and are believed to have been even more numerous at earlier times.[3] The large

---

[1] We note that for this density profile, the enclosed mass integral cannot be solved analytically and we will perform numerical estimates.

[2] This approach follows the analysis of Schive et al. (2014a,b) that found the soliton to be a good approximation of the full density profile. Marsh & Pop (2015) included the NFW component and found that it was unconstrained, and the data could be fit using only the soliton.

[3] This is not necessarily the case in the ψDM model, where structure formation is not strictly hierarchical because of the mass function cut-off.

mass-to-light ratios of dwarf galaxies, and in particular of ultra-faint dwarfs (half-light radius $\lesssim 50$ pc), suggest that they are the most DM-dominated objects and therefore a great laboratory to test DM models.

The richest source of information are nearby dwarfs, e.g. the Milky Way dwarf satellites, where individual stars can be resolved and stellar dynamics can track the density profile and the gravitational field. A candidate object identified in a survey can be considered a dwarf galaxy, and distinguished from stellar clusters, if it shows a velocity dispersion in excess of what would be expected from stellar mass alone (~ 0.3 km s^{-1}) or a dispersion in stellar metallicity ($\gtrsim 0.1$ dex in iron) indicating chemical self-enrichment (Willman & Strader 2012). These two properties make the candidate a dwarf galaxy dominated by dark matter.

In the last two decades, many faint dwarf galaxies have been discovered with photometric surveys [SDSS (Belokurov et al. 2007), DES (Bechtol et al. 2015; Drlica-Wagner et al. 2015; Koposov et al. 2015)]. Here, we consider newly discovered ultra-faint dwarf galaxies, Draco II and Triangulum II, with the Pan-STARRS1 3π survey (Laevens et al. 2015a,b).

(i) Draco II
Draco II discovery (Laevens et al. 2015b) reported a close (distance from the Sun 20 ± 3 kpc), extremely compact (half-light radius $r_h = 19^{+8}_{-6}$ pc) and faint ($L_{\odot} = 10^{3.1 \pm 0.3}$) object whose nature was uncertain. The addition of spectroscopic observations led Martin et al. (2016a) to find a small, yet marginally detected, velocity dispersion, $\sigma_{vr} = 2.9 \pm 2.1$ km s^{-1}, and a highly sub-solar metallicity, [Fe/H] < −2.1. Draco II stellar dynamics constrain the half-light mass to be $\log_{10}(M_{1/2}) = 5.5^{+0.4}_{-0.6}$ and a mass-to-light ratio $\log_{10}((M/L)_{1/2}) = 2.7^{+0.5}_{-0.8}$ (Martin et al. 2016a, using the definition of $M_{1/2}$ presented in Wolf et al. 2010). These estimates hint to a strongly dark matter dominated system and in particular to the smallest compact dwarf galaxy ever confirmed.

(ii) Triangulum II
Similarly to Draco II, Triangulum II photometric properties were first reported in Laevens et al. (2015a) and then followed-up with a spectroscopic analysis in Kirby et al. (2015) and Martin et al. (2016b). Triangulum II is a larger ($r_h = 34^{+9}_{-8}$ pc) but fainter ($L_{\odot} = 10^{2.6 \pm 0.2}$) system located at 30 ± 2 kpc. The velocity dispersion of the member stars was found to be $\sigma_{vr} = 5.1^{+4.0}_{-1.4}$ km s^{-1} with a corresponding $\log_{10}(M_{1/2}) = 5.9^{+0.4}_{-0.2}$ and $(M/L)_{1/2} = 3600^{+3500}_{-2100}$ in solar units (Kirby et al. 2015). As for Draco II, these estimates (together with very low metallicity, [Fe/H] = −2.5 ± 0.8) suggest that Triangulum II is a dwarf galaxy. A later analysis by Martin et al. (2016b) reported somehow different results ($\sigma_{vr} = 9.9^{+3.2}_{-2.2}$ km s^{-1}, $M_{1/2} \sim 3 \times 10^6$ M$_{\odot}$, $(M/L)_{1/2} \sim 15\,500$) with inner and outer stars' velocities in slight disagreement and with the nature of Triangulum II more uncertain. With current data, the uncertainty on these numbers is too big to have statistical significance and therefore we choose to continue our analysis assuming Triangulum II is a faint dwarf galaxy and using the estimates in Kirby et al. (2015). Both analyses, however, highlight that Triangulum II has a very large mass-to-light ratio, classifying it as the most DM dominated dwarf galaxy ever observed.

4 M22 ESTIMATE

To estimate the DM particle mass, we match enclosed mass predictions with the observed half-light masses; fitting theoretical haloes to half-light measurements of satellite galaxies has been widely done in the literature to investigate different density profiles (see e.g. Collins et al. 2014; Brook & Di Cintio 2015).

Schive et al. (2014a) and Marsh & Pop (2015) constrained the DM particle mass performing a simplified Jeans analysis on the resolved stellar populations of Fornax and analysing the mass profile slopes of Fornax and Sculptor dwarfs, respectively. A full Jeans analysis using the standard eight Milky Way dwarf satellite galaxies to estimate m_{22} (which is indeed a universal parameter) will soon appear in Gonzalez-Morales et al., in preparation. The galaxies we consider here are very faint and observations do not have the needed resolution to better resolve the stellar dynamics (e.g. no information on velocity anisotropy). Our calculations are then preliminary estimates of the DM component and we defer a more extensive analysis to future data.

We use the following two observational limits.

(i) The half-light mass, $M_{1/2}$
We assume that the stellar populations observed in Draco II and Triangulum II are within the respective core radius and we use the $M_{1/2}$ measurements to anchor the enclosed mass profile:

$$M_{1/2} = \int_0^{r_{1/2}} \frac{4\pi 1.9(10 m_{22})^{-2} r_c^{-4} r'^2}{[1 + 9.1 \times 10^{-2}(r'/r_c)^2]^8} \mathrm{d}r' 10^9 \,\mathrm{M}_{\odot}, \qquad (5)$$

where $r_{1/2} = 4/3 r_h$ is the 3D deprojected half-light radius (Wolf et al. 2010).

This assumption is a good approximation with the current resolution, in both cases only very few stars are resolved (nine in Draco II and six in Triangulum II) and they seem to be in a single stellar system.

(ii) The maximum halo mass, M_h^{max}
We impose a maximum halo mass based on the mass function of the Milky Way dwarf satellite galaxies (Giocoli, Tormen & van den Bosch 2008). We choose M_h^{max} to be $10^{-2} M_{MW} \sim 2 \times 10^{10}$ M$_{\odot}$. Such a maximum halo mass for satellites is in agreement with recent Local Group abundance matching results (Brook et al. 2014). Moreover, $M_h^{max} >$ few $\times 10^{10}$ M$_{\odot}$ are forbidden by dynamical friction time-scales limits (Gerhard & Spergel 1992).

We fold this into equation (4) and get

$$m_{22} = \frac{1.6}{r_c} \left(\frac{M_h^{max}}{10^9 \,\mathrm{M}_{\odot}} \right)^{-1/3}. \qquad (6)$$

We will discuss later how the results change had we chosen a different M_h^{max}.

4.1 Numerical results

We can now combine equations (5) and (6) and numerically estimate the two parameters of the model ($r_c - m_{22}$) for the two galaxies. We find:

$$r_c \sim 105 \text{ pc}; \ m_{22} \sim 5.6 \qquad (7)$$

for Draco II and

$$r_c \sim 160 \text{ pc}; \ m_{22} \sim 3.8 \qquad (8)$$

for Triangulum II.

The corresponding core masses, using equation (3), are $M_c^{DraII} \sim 1.5 \times 10^7$ M$_{\odot}$ and $M_c^{TriII} \sim 2.3 \times 10^7$ M$_{\odot}$.

We show the ψDM model predictions using these estimates and the half-light mass data in Fig. 1. The plot also shows NFW predictions for different values of the halo mass. In an NFW model, these ultra-faint dwarfs lie systematically high compared to what we would expect, $M_h \approx 10^8$–10^{10} M$_{\odot}$ (see also fig. 6 in Martin
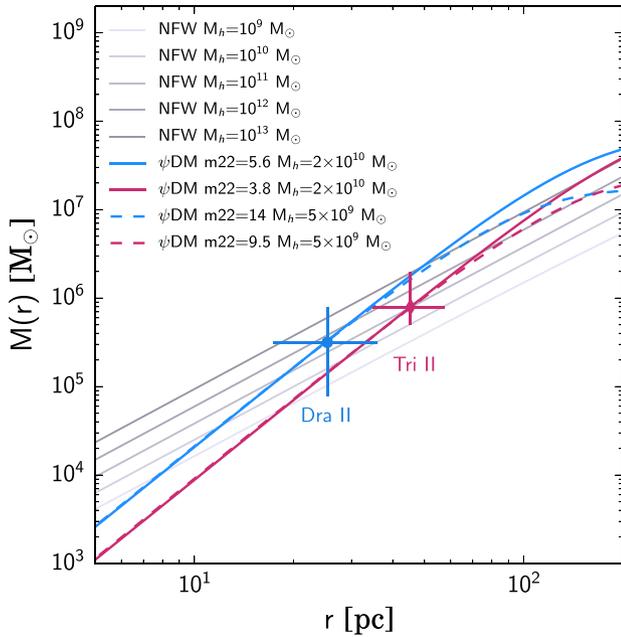
Figure 1. Half-light mass measurements at the 3D deprojected half-light radius for Draco II (Martin et al. 2016a) and Triangulum II (Kirby et al. 2015). Grey lines, from lighter to darker, show predictions for the enclosed mass in a ΛCDM NFW model with M_h going from 10^9 to 10^{13} M$_\odot$. The NFW profiles are built using the scaling relations between the concentration parameter and the halo mass derived in Macciò, Dutton & van den Bosch (2008) and updated in Dutton & Macciò (2014) for the *Planck* 2013 cosmology (Planck Collaboration XVI 2014) [Equation (8) of Dutton & Macciò 2014]. Solid coloured lines show the estimated enclosed mass for the ψDM model with $r_c \sim 105$pc - $m_{22} \sim 5.6$ for Draco II and $r_c \sim 160$pc - $m_{22} \sim 3.8$ for Triangulum II. For the ψDM model, we compute only the soliton mass as total enclosed mass, this is a good approximation assuming that the stellar populations are within the core and that the soliton extends to ~3 core radii (Schive et al. 2014a,b). As a comparison, in dashed coloured lines, we report ψDM estimates for a less massive hosting halo; in the ψDM model we can easily reconcile the data with smaller haloes at the expenses of a more massive DM particle.

et al. 2016b). However, given the uncertainty on these measurements, the data points seem to agree with a wide range of values for the halo mass; all models with $M_h \approx 10^9$–10^{13} M$_\odot$ are within the 1σ errorbar and no definitive conclusion can be drawn. This plot is in fact highlighting an intrinsic limitation of constraining mass profiles with the innermost regions of galaxies. As shown in Ferrero et al. (2012), different theoretical predictions lie very close to each other at very small radii ($r < 1$ kpc) and a wide range of models agree with the data. To break the models degeneracy, observations of stars outside the core, constraining the velocity dispersion – or equivalently the mass – at larger radii are needed. Nevertheless, the higher NFW curves conflict with physical constraints, M_h cannot reach the same mass of the host galaxy (the Milky Way in this case) and cannot be bigger than the limits imposed by dynamical friction. In the case of ψDM, we avoid this by imposing in the parameters model extraction the M_h^{max} quantity and finding a lower bound on m_{22} corresponding to the maximum mass we allow for the halo. If we choose a lower value for M_h^{max}, e.g. ~5×10^9 M$_\odot$, the estimates become $r_c \sim 66$ pc – $m_{22} \sim 14$ – $M_c \sim 3.8 \times 10^6$ M$_\odot$ for Draco II and $r_c \sim 99$ pc – $m_{22} \sim 9.5$ – $M_c \sim 5.7 \times 10^6$ M$_\odot$ for Triangulum II. This means that our estimates for m_{22} in the case of $M_h^{max} = 2 \times 10^{10}$ M$_\odot$ are lower limits for the DM particle mass.
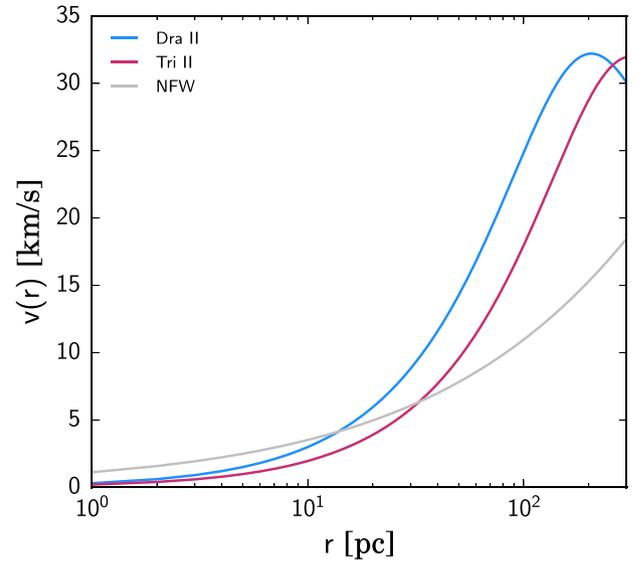

Figure 2. Circular velocity distribution predicted using the ψDM model estimates for Draco II (blue line) and Triangulum II (magenta line) and using an NFW density profile with a 2×10^{10} M$_\odot$ halo mass.

In the ψDM model, we can easily reconcile the data with smaller haloes at the expenses of a more massive DM particle.

We want to stress that in these results we are strongly dominated by the anticorrelation between r_c and m_{22} (see fig. S4 in Schive et al. 2014a), deeper observations, resolving multiple stellar systems positioned at different radii in the enclosed mass predictions, will be fundamental to get more robust estimates.

We report in Fig. 2 the predicted circular velocities, $v(r) = \sqrt{(GM(<r)/r)}$, out to three times the core radius – where the soliton density is a good approximation of the total halo density – for the ψDM estimates derived above and for an NFW profile with the same M_h^{max}. As previously anticipated, the plot highlights that measurements of the stellar velocities at larger distances from the centre will help distinguish between different curves and impose strong constraints on the density profiles. We note that this plot does not extend to the constant velocity regime generated by the additional NFW-like density profile term overtaking the soliton profile at large scales.

5 DISCUSSION

In this paper, we have estimated the dark matter particle mass from newly discovered ultra-faint dwarf galaxies in a scenario where dark matter is made of ultra-light bosons, axion-like particles, condensate in a coherent wave.

Wave Dark Matter (ψDM) has recently been a very valuable alternative to CDM to solve the small-scale crisis of CDM in galaxy formation (Schive et al. 2014a,b, 2016; Marsh & Pop 2015). The ψDM model in fact superpose a soliton core depending on the DM particle mass m on an NFW density profile, smoothing the unwanted cusp in the centre of the density profile and suppressing formation of haloes smaller than 10^{10} M$_\odot$. At large scales, ψDM clustering is statistically indistinguishable from CDM.

We have considered in this work, data from recently discovered Draco II and Triangulum II Milky Way dwarf satellites. The measurements of the luminosity of these objects suggest that they are systems with a mass-to-light ratio of ~10^7 in the outer regions and

therefore completely DM dominated. With such extreme DM environments, these dwarfs provide a great laboratory to study dark matter physics despite the contribution of baryonic feedback.

We anchor the soliton density profile of the ψDM model using Draco II and Triangulum II half-light mass measurements and limits from the halo mass function of Milky Way satellite galaxies, and estimate at the same time the core radius r_c and the DM particle mass m. We find that the ψDM model requires $r_c \sim 105$ pc - $m \sim 5.6 \times 10^{-22}$ eV for Draco II and $r_c \sim 160$ pc - $m \sim 3.8 \times 10^{-22}$ eV for Triangulum II. With these values of the parameters, the haloes hosting the galaxies have a total mass of 2×10^{10} M$_\odot$. If we impose a smaller halo mass, we can readjust the estimates of r_c and m and embed these dwarfs in less massive haloes with a smaller core radius and a more massive DM particle.

Ultra-light axion-like particles have been recently tested with many cosmological probes as an alternative to CDM and the interesting scenario of many data supporting 10^{-23} eV $\lesssim m \lesssim 10^{-21}$ eV is lately emerging: Lyman α systems constraints are presented in Amendola & Barbieri (2006), galaxy formation, galaxy dynamics, and UV luminosity function tests in Lora & Magaña (2014); Lora (2015), Schive et al. (2014a, 2016), Marsh & Pop (2015); Marsh & Silk (2014), reionization constraints in Bozek et al. (2015), Sarkar et al. (2016), and CMB limits in Hlozek et al. (2015). Our estimates fit very nicely into these bounds and highlight how promising ultra-faint dwarf galaxies are in testing DM models.

Deeper observations from future experiments like JWST (Gardner et al. 2006), WFRIST (Spergel et al. 2013), LSST (LSST Science Collaboration et al. 2009), and Euclid (Laureijs et al. 2011) will enable further discoveries of Milky Way satellites and will characterize the stellar systems within these dwarfs with the resolution needed for more detailed analysis. They will, for example, enable some potential tests for the ψDM model:

(i) *minimum halo mass* – Following Schive et al. (2014a,b) we can estimate the minimum halo mass possible in this scenario, $M_h^{min} \sim 4.4 \times 10^7 m_{22}^{-3/2} \sim 5 \times 10^6$ M$_\odot$. These objects will be the target of sub-haloes detection via milli-lensing (Dalal & Kochanek 2002) and strong-lensing (Hezaveh et al. 2014).

(ii) *late galaxy formation* – Lyman α emission, galaxy luminosity function (from JWST), and reionization (from CMB (Calabrese et al. 2014) or 21 cm (Kadota et al. 2014)) will test the suppression of galaxy formation at high redshift predicted by this model (Marsh & Silk 2014; Schive et al. 2016).

(iii) *sub-halo masses* – The halo mass function will manifest a truncation at low masses in the case of ψDM (Marsh & Silk 2014; Schive et al. 2016), with a suppression of objects below the Jeans scale set by the DM particle mass. Moreover, considering that our knowledge of the Galactic plane will soon dramatically improve with *Gaia* (Perryman et al. 2001), we can test this natural cut-off of the model by observing the predicted suppression of tidal streams.

ACKNOWLEDGEMENTS

REFERENCES

Amendola L., Barbieri R., 2006, Phys. Lett. B, 642, 192
Bechtol K. et al., 2015, ApJ, 807, 50
Belokurov V. et al., 2007, ApJ, 654, 897
Blumenthal G. R., Faber S. M., Primack J. R., Rees M. J., 1984, Nature, 311, 517
Böhmer C. G., Harko T., 2007, J. Cosmol. Astropart. Phys., 6, 25
Bozek B., Marsh D. J. E., Silk J., Wyse R. F. G., 2015, MNRAS, 450, 209
Brook C. B., Di Cintio A., 2015, MNRAS, 450, 3920
Brook C. B., Di Cintio A., Knebe A., Gottlöber S., Hoffman Y., Yepes G., Garrison-Kimmel S., 2014, ApJ, 784, L14
Calabrese E. et al., 2014, J. Cosmol. Astropart. Phys., 8, 010
Chavanis P.-H., 2011, Phys. Rev. D, 84, 043531
Chavanis P. H., 2012, A&A, 537, A127
Chavanis P.-H., Delfini L., 2011, Phys. Rev. D, 84, 043532
Collins M. L. M. et al., 2014, ApJ, 783, 7
Dalal N., Kochanek C. S., 2002, ApJ, 572, 25
Davidson S., 2015, Astropart. Phys., 65, 101
Di Cintio A., Brook C. B., Macciò A. V., Stinson G. S., Knebe A., Dutton A. A., Wadsley J., 2014, MNRAS, 437, 415
Drlica-Wagner A. et al., 2015, ApJ, 813, 109
Dutton A. A., Macciò A. V., 2014, MNRAS, 441, 3359
Ferrero I., Abadi M. G., Navarro J. F., Sales L. V., Gurovich S., 2012, MNRAS, 425, 2817
Gardner J. P. et al., 2006, Space Sci. Rev., 123, 485
Gerhard O. E., Spergel D. N., 1992, ApJ, 389, L9
Giocoli C., Tormen G., van den Bosch F. C., 2008, MNRAS, 386, 2135
Goodman J., 2000, New Astron., 5, 103
Governato F. et al., 2012, MNRAS, 422, 1231
Guth A. H., Hertzberg M. P., Prescod-Weinstein C., 2015, Phys. Rev. D, 92, 103513
Guzmán F. S., Lora-Clavijo F. D., 2015, Gen. Relativ. Gravit., 47, 21
Guzmán F. S., Matos T., Villegas H. B., 1999, Astron. Nachr., 320, 97
Harko T., 2011a, J. Cosmol. Astropart. Phys., 5, 22
Harko T., 2011b, Phys. Rev. D, 83, 123515
Harko T., 2014, Phys. Rev. D, 89, 084040
Harko T., Lobo F. S. N., 2015, Phys. Rev. D, 92, 043011
Harko T., Madarassy E. J. M., 2012, J. Cosmol. Astropart. Phys., 1, 20
Harko T., Mocanu G., 2012, Phys. Rev. D, 85, 084012
Harko T., Liang P., Liang S.-D., Mocanu G., 2015, J. Cosmol. Astropart. Phys., 11, 27
Hezaveh Y., Dalal N., Holder G., Kisner T., Kuhlen M., Perreault Levasseur L., 2014, preprint (arXiv:1403.2720)
Hlozek R., Grin D., Marsh D. J. E., Ferreira P. G., 2015, Phys. Rev. D, 91, 103512
Hu W., Barkana R., Gruzinov A., 2000, Phys. Rev. Lett., 85, 1158
Ji S. U., Sin S. J., 1994, Phys. Rev. D, 50, 3655
Kadota K., Mao Y., Ichiki K., Silk J., 2014, J. Cosmol. Astropart. Phys., 6, 011
Kirby E. N., Cohen J. G., Simon J. D., Guhathakurta P., 2015, ApJ, 814, L7
Koposov S. E., Belokurov V., Torrealba G., Evans N. W., 2015, ApJ, 805, 130
Kuhlen M., Vogelsberger M., Angulo R., 2012, Phys. Dark Universe, 1, 50
Laevens B. P. M. et al., 2015a, ApJ, 802, L18
Laevens B. P. M. et al., 2015b, ApJ, 813, 44
Laureijs R. et al., 2011, preprint (arXiv:1110.3193)
Lee J.-W., Koh I.-G., 1996, Phys. Rev. D, 53, 2236
Li B., Rindler-Daller T., Shapiro P. R., 2014, Phys. Rev. D, 89, 083536
Lora V., 2015, ApJ, 807, 116
Lora V., Magaña J., 2014, J. Cosmol. Astropart. Phys., 9, 11
Lora V., Magaña J., Bernal A., Sánchez-Salcedo F. J., Grebel E. K., 2012, J. Cosmol. Astropart. Phys., 2, 11
LSST Science Collaboration et al., 2009, preprint (arXiv:0912.0201)
Lundgren A. P., Bondarescu M., Bondarescu R., Balakrishna J., 2010, ApJ, 715, L35
Macciò A. V., Dutton A. A., van den Bosch F. C., 2008, MNRAS, 391, 1940
Magaña J., Matos T., 2012, J. Phys. Conf. Ser., 378, 012012
Marsh D. J. E., 2015a, preprint (arXiv:1510.07633)
Marsh D. J. E., 2015b, Phys. Rev. D, 91, 123520
Marsh D. J. E., Pop A.-R., 2015, MNRAS, 451, 2479
Marsh D. J. E., Silk J., 2014, MNRAS, 437, 2652

Martin N. F. et al., 2016a, MNRAS, 458, L59

Martin N. F. et al., 2016b, ApJ, 818, 40

Matos T., Guzmán F. S., Ureña-López L. A., 2000, Class. Quantum Gravity, 17, 1707

Navarro J. F., Frenk C. S., White S. D. M., 1996, ApJ, 462, 563

Oñorbe J., Boylan-Kolchin M., Bullock J. S., Hopkins P. F., Kereš D., Faucher-Giguère C.-A., Quataert E., Murray N., 2015, MNRAS, 454, 2092

Papastergis E., Shankar F., 2015, preprint (arXiv:1511.08741)

Pawlowski M. S., Famaey B., Merritt D., Kroupa P., 2015, ApJ, 815, 19

Perryman M. A. C. et al., 2001, A&A, 369, 339

Planck Collaboration XVI, 2014, A&A, 571, A16

Planck Collaboration XIII, 2015, preprint (arXiv:1502.01589)

Pontzen A., Governato F., 2014, Nature, 506, 171

Sarkar A., Mondal R., Das S., Sethi S. K., Bharadwaj S., Marsh D. J. E., 2016, J. Cosmol. Astropart. Phys., 4, 012

Schive H.-Y., Chiueh T., Broadhurst T., 2014a, Nature Phys., 10, 496

Schive H.-Y., Liao M.-H., Woo T.-P., Wong S.-K., Chiueh T., Broadhurst T., Hwang W.-Y. P., 2014b, Phys. Rev. Lett., 113, 261302

Schive H.-Y., Chiueh T., Broadhurst T., Huang K.-W., 2016, ApJ, 818, 89

Sikivie P., Yang Q., 2009, Phys. Rev. Lett., 103, 111301

Spergel D. N. et al., 2003, ApJS, 148, 175

Spergel D. et al., 2013, preprint (arXiv:1305.5422)

Suárez A., Robles V. H., Matos T., 2014, Astrophys. Space Sci. Proc. Vol. 38, Accelerated Cosmic Expansion. Springer International Publishing, Switzerland, p. 107

Turner M. S., 1983, Phys. Rev. D, 28, 1243

Weinberg D. H., Bullock J. S., Governato F., Kuzio de Naray R., Peter A. H. G., 2013, preprint (arXiv:1306.0913)

White S. D. M., Frenk C. S., 1991, ApJ, 379, 52

White S. D. M., Rees M. J., 1978, MNRAS, 183, 341

Widrow L. M., Kaiser N., 1993, ApJ, 416, L71

Willman B., Strader J., 2012, AJ, 144, 76

Wolf J., Martinez G. D., Bullock J. S., Kaplinghat M., Geha M., Muñoz R. R., Simon J. D., Avedo F. F., 2010, MNRAS, 406, 1220

Woo T.-P., Chiueh T., 2009, ApJ, 697, 850

This paper has been typeset from a TEX/LATEX file prepared by the author.